Role of Projectile and Surface Temperatures in the Energy Transfer Dynamics of Protonated Peptide Ion Collisions with the Diamond {111} Surface†

Asif Rahaman,‡ Othalene Collins,§ Chavell Scott,§ Jiangping Wang,§ and William L. Hase*,‡

Department of Chemistry and Biochemistry, Texas Tech University, Lubbock, Texas 79409-1061, and Department of Chemistry, Wayne State University, Detroit, Michigan 48202

Received: December 8, 2005; In Final Form: May 8, 2006

The effects of temperature on energy transfer during collisions of protonated diglycine ions, Gly_2-H^+, with a diamond {111} surface were investigated by chemical dynamics simulations. The simulations were performed for a collision energy of 70 eV and angle of 0° with respect to the surface normal. In one set of simulations the initial surface temperature, T_{surf}, was varied from 300 to 2000 K, while the Gly_2-H^+ vibrational and rotational temperatures were maintained at 300 K. For the second set of simulations the Gly_2-H^+ vibrational temperature, T_{vib}, was varied from 300 to 2000 K, keeping both the Gly_2-H^+ rotational and surface temperatures at 300 K. Increasing either the surface temperature or Gly_2-H^+ vibrational temperature to values as high as 2000 K has, at most, only a negligible effect on the partitioning of the incident collision energy to the surface and to the vibrational and rotational modes of Gly_2-H^+. To a good approximation, the initial surface and peptide ion energies are nearly adiabatic during the collisional energy transfer. This adiabaticity of the initial peptide ion energy agrees with experiments (*J. Phys. Chem. A* **2004**, *108*, 1). A more quantitative analysis of the effects of T_{vib} and T_{surf} shows there are small, but noticeable, effects on the energy transfer efficiencies. Namely, increasing the vibrational or surface temperature results in a near-linear decrease in the energy transfer to the degrees of freedom associated with this temperature.

I. Introduction

There is a considerable interest in the chemical dynamics associated with surface-induced dissociation (SID),[1,2] which is a very important mass spectrometric technique for determining structural properties of ions and both energies and mechanistic pathways[3−7] for their dissociation. The fragmentation products from SID are a fingerprint of the ion's structure, and SID may be used to identify the amino acid sequence of a protonated peptide ion.[4,8−17] In a typical SID experiment, a projectile ion with a fixed translation energy (E_i) and incident angle (θ_i) is collided with a surface. During the collision, part of the ion's translation energy is converted into surface vibration (ΔE_{surf}) and internal vibration/rotation degrees of freedom (ΔE_{int}) of the ion such that

$$E_i = E_f + \Delta E_{surf} + \Delta E_{int} \quad (1)$$

where E_f is the final translation energy after the collision. This energy transfer model assumes the collisions are electronically adiabatic, and excitation of the electronic states of either the projectile or surface is unimportant. This model is consistent with SID experiments involving peptide ions and hydrocarbon surfaces, which do not have low-lying electronic states.[1,2,10,13,14,17] Understanding the energy transfer dynamics of SID is of fundamental, as well as practical, interest.

To interpret SID experiments, it is important to know the distributions of energy transferred to the surface, $P(\Delta E_{surf})$; to the scattered ion's internal vibration/rotation degrees of freedom, $P(\Delta E_{int})$; and of energy remaining in projectile translation, $P(E_f)$. Several methods have been developed to measure $P(\Delta E_{int})$.[18−21] Experimental results indicate that the efficiency of energy transfer to the ion depends on several factors, including surface composition,[22−25] projectile structure,[10] collision energy,[5,16,26] and incident angle.[5,16,27] In a different interpretation of the experiments, Kubišta et al.[19] suggested that the fraction of E_i transferred to the projectile's internal energy is nearly independent of the incident angle.

Classical trajectory simulations, based on accurate potential-energy surfaces, have proven to be an important method for determining distributions of energy transfer in SID.[16] For Cr^+-$(CO)_6$ SID on a *n*-hexylthiolate self-assembled monolayer (H-SAM), the ΔE_{int} energy transfer distribution determined from a simulation[28] is in quantitative agreement with experiment.[25] Simulations of energy transfer in protonated glycine, triglycine, and pentaglycine SID give ΔE_{int} energy transfer distributions similar to those determined from experiments for protonated dialanine.[17] In simulations of protonated diglycine (Gly_2-H^+) with diamond {111}, Wang et al.[29] varied the incident angle from 0° to 45° and observed a small decrease in transfer to the peptide's internal degrees of freedom, ΔE_{int}, and a larger decrease in transfer to the surface, ΔE_{surf}, while substantially more energy remained in E_f. The dependence of the energy transfer to ΔE_{int}, ΔE_{surf} and E_f on θ_i observed in these simulations, are in qualitative agreement with experiments by Herman and co-workers.[19,30]

In this article, quasiclassical trajectory simulations are reported for the energy-transfer dynamics associated with scattering of Gly_2-H^+ off diamond {111}. The temperatures of this surface and of Gly_2-H^+ are varied to determine their effects on the energy transfer dynamics. The trajectory simulations are carried out at a collision energy of 70 eV and collision angle of 0° with respect to the surface normal. In one set of simulations,

* To whom correspondence should be addressed: e-mail bill.hase@ttu.edu.
† Part of the "Chava Lifshitz Memorial Issue".
‡ Texas Tech University.
§ Wayne State University.

10.1021/jp057159o CCC: $33.50 © 2006 American Chemical Society
Published on Web 06/08/2006

the surface temperature is varied while both the rotational and vibrational temperatures of Gly_2-H^+ are kept at 300 K. In the second set of simulations, the vibrational temperature of Gly_2-H^+ is varied while the surface temperature and Gly_2-H^+ rotational temperature are maintained at 300 K. For the different temperatures, average percentages are determined for the transfer of the collision energy to the Gly_2-H^+ internal degrees of freedom, E_{int}, and to the surface, E_{surf}, as well as for the amount remaining in translation, E_f. Distributions are also determined for ΔE_{int}, ΔE_{surf}, and E_f. The effect of the projectile vibrational temperature on the energy transfer is compared with experiments.

II. Potential Energy Function

The potential-energy function used for the simulations is expressed as

$$V = V_{ion} + V_{surf} + V_{ion,surf} \quad (2)$$

where V_{ion} is the Gly_2-H^+ intramolecular potential, V_{surf} is the potential for diamond {111}, and $V_{ion,surf}$ is the intermolecular potential between Gly_2-H^+ and the surface. The AMBER 94[31] molecular mechanical (MM) model was used for V_{ion}. Previous work has shown that this model for V_{ion} gives the same energy transfer dynamics as does the AM1 semiempirical quantum mechanical (QM) model.[32]

The potential for diamond {111} is similar to that reported earlier.[28] The diamond surface model is hydrogen-terminated with eight layers of carbon atoms and a total of 1988 atoms. A "slab" model of this size for the surface gives results in very good agreement with experiment.[17,33,34] The surface area of the model is 34 Å × 34 Å and its thickness is 8 Å, from the top hydrogen atoms to the bottom carbon atoms (see Figure 1 in ref 28). Five massive atoms are added to the bottom corner and middle of the model to ensure it does not move when the surface is hit by Gly_2-H^+. The mass is sufficiently large that even if all of the collision energy is transferred to one of these atoms, the atom would move negligibly during the simulation. The potential energy function for diamond {111} consists of harmonic stretches and bends, with force constants chosen to fit the phonon spectrum of diamond.[35]

The peptide/surface intermolecular potential is modeled by a sum of two body potentials between the atoms of the peptide ion and surface, which are expressed as

$$V_{xy} = A_{xy} \exp(-B_{xy}R_{xy}) + C_{xy}/R_{xy}^6 \quad (3)$$

where the subscript x corresponds to the C or H of the diamond surface and the subscript y corresponds to the H, C, O, and N atoms of the peptide. The AMBER force field[31] was developed to represent the long-range components of these intermolecular interactions, including the potential minima. However, it was not developed to represent the short-range repulsive regions of the intermolecular potentials, which affect the Gly_2-H^+/diamond {111} energy transfer dynamics. Previous work[36] has shown that it is necessary to have proper models for these repulsive potentials to determine reliable energy transfer efficiencies from the simulations. Accurate repulsive intermolecular potentials were developed, from ab initio calculations, for protonated polyglycine and polyalanine ions interacting with diamond {111}.[34] The parameters A_{xy}, B_{xy}, and C_{xy} in eq 3 were determined by nonlinear least-squares fits of ab initio potential energies calculated between CH_4, as a model for the C and H atoms of the surface, and CH_4, NH_3, NH_4^+, H_2CO, and H_2O, as models for the different types of atoms and functional groups of the peptide ions.

III. Computational Procedure

The classical trajectory simulations were carried out with the general chemical dynamics package VENUS.[37] Initial conditions[28] were chosen to determine effects of the energy transfer distributions on the temperature of the surface and on the vibrational temperature of the peptide ion. The center of a beam of peptide ions is aimed at the center of the surface with a fixed initial translational energy, E_i, of 70 eV and a fixed incident angle, θ_i, of 0° with respect to the surface normal. The radius of the beam is chosen so that the beam overlaps a hexagonal repeating unit on the top of the surface[28] with an area of 16.4 Å^2. The trajectory results are insensitive to its radius. The projectile for each trajectory is randomly placed in the cross-section of this beam and randomly rotated about its center of mass so that it has an initial random orientation with respect to the surface. The azimuthal angle, χ, between the beam and a fixed plane perpendicular to the surface is sampled randomly between 0 and 2π. Such a random sampling of χ simulates collisions with different domains of growth on the surface.[28] The distance between the center of the beam and the center of the top of the surface is set to 25 Å.

The initial conditions for the vibrational modes of the peptide ions are chosen via the quasiclassical normal mode method,[38−40] which includes zero-point energy (ZPE). The energy, for each normal mode of vibration, is selected from the quantum harmonic oscillator Boltzmann distribution corresponding to a vibrational temperature (T_{vib}) of the peptide ion. The energy is randomly partitioned between the kinetic and potential energies by choosing a random phase for each normal mode. A rotational energy of $RT/2$ corresponding to a temperature of 300 K is added to each principal axis of rotation of the peptide.

Initial conditions for the surface, representing a Boltzmann distribution at a temperature T_{surf}, were determined from a 1 ps molecular dynamics simulation, in which the atomic velocities are scaled[41] to correspond to T_{surf}. The structure and velocities obtained from this equilibration are then used as the initial conditions for an equilibration run at the beginning of each trajectory. A time step of 0.2 fs is used to integrate the classical equation of motion, which provided energy conservation of 0.2 kcal/mol or less. This is much smaller than the amounts of collision energy transferred to the surface and Gly_2-H^+ (see below).

The trajectories are calculated with surface temperatures, T_{surf}, of 300, 1000, 1500, and 2000 K while the vibrational (T_{vib}) and rotational (T_{rot}) temperatures of the peptide are held at 300 K. Then, while both T_{surf} and T_{rot} are kept at 300 K, T_{vib} is varied from 300 to 2000 K. Five hundred trajectories are calculated for each set of initial conditions. When a trajectory is terminated, the peptide ion's final translational energy, E_f, is determined. The peptide ion's internal energy change, ΔE_{int}, is determined by subtracting the initial value of the projectile's internal energy from its final value. The surface internal energy change, ΔE_{surf}, is determined similarly. These final energies show how the peptide ion's collision energy is transferred.

The 70 eV collision energy corresponds to 1614 kcal/mol, which is much larger than the initial internal energy of the peptide ion but smaller than the initial energy of the "slab" model for the surface. For the trajectories calculated at T_{vib} = 300, 1000, 1500, and 2000 K, the average quasiclassical internal energies of Gly_2-H^+, including zero-point energy, are 94.5, 133.5, 172.2, and 214.9 kcal/mol, respectively. If the initial

TABLE 1: Effects of Surface and Peptide Ion Vibrational Temperatures on Collision Energy Transfer with the Diamond {111} Surface[a]

T_{rot} (K)	T_{vib} (K)	T_{surf} (K)	ΔE_{int}	ΔE_{surf}	E_f
300	300	300	20.3 (0.4)	37.6 (0.3)	42.1 (0.2)
300	300	1000	21.0 (0.4)	36.5 (0.3)	42.5 (0.2)
300	300	1500	21.3 (0.4)	36.6 (0.3)	42.1 (0.2)
300	300	2000	21.7 (0.4)	35.8 (0.3)	42.4 (0.2)
300	1000	300	19.7 (0.4)	38.2 (0.3)	42.1 (0.2)
300	1500	300	19.7 (0.4)	38.6 (0.3)	42.3 (0.2)
300	2000	300	18.8 (0.4)	39.0 (0.3)	42.2 (0.2)

[a] Average percents of the collision energy transferred to protonated diglycine internal energy (ΔE_{int}), the surface (ΔE_{surf}), and peptide translation (E_f) for protonated diglycine collisions with the diamond {111} surface at different vibrational temperatures, T_{vib}, of the peptide and temperatures of the surface, T_{surf}. The collision energy is 70 eV and the collision angle is 0°. The standard deviation of the mean obtained from 500 trajectories is given in parentheses.

energies for the Gly_2-H^+ normal modes had been sampled classically, with an average energy of *RT* for each mode, the average energies of Gly_2-H^+ for the above respective temperatures would be 28.6, 95.4, 143.1, and 190.8 kcal/mol. For the trajectories calculated, the initial total energy for the slab model of the surface varies from 3752 to 23 760 kcal/mol as the surface temperature is increased from 300 to 2000 K. However, these latter energies are not particularly meaningful since the slab model used here gives good agreement with experiment[15,33] and is expected to give the same energy transfer results as those for a much larger slab model approaching a macroscopic object.[42]

IV. Trajectory Results

A. Effects of Surface Temperature. Values of the average percent energy transfers of the collision energy to E_{int} and E_{surf} and the percent remaining in translation, E_f, are listed in Table 1 for the simulations at different surface temperatures, while T_{vib} and T_{rot} of Gly_2-H^+ were held at 300 K. Overall, these percentages are at most only weakly dependent on T_{surf}. The majority of the collision energy remains in Gly_2-H^+ translation, with E_f accounting for ~42% of the collision energy, a percentage that is independent of T_{surf}. However, as shown in Figure 1, there is a small, near-linear increase and decrease in the transfer of energy to ΔE_{int} and ΔE_{surf}, respectively, as T_{surf} is increased. Thus, there are small, but detectable effects in the energy transfer efficiencies with increase in T_{surf}.

The distributions for the final energies, $P(\Delta E_{int})$, $P(\Delta E_{surf})$, and $P(E_f)$, are plotted in Figure 2 for simulations with T_{surf} of 300 and 2000 K. The standard deviations for the distributions are given as error bars in the form of vertical lines. The distributions for the two different temperatures are nearly similar in shape. However, a more careful inspection shows that as T_{surf} is increased, the peaks in $P(\Delta E_{int})$ and $P(\Delta E_{surf})$ slightly shift to higher and lower values, respectively. In contrast, there is no change in the $P(E_f)$ peak. These small shifts affect the energy transfer efficiencies. Thus, the increase in the surface temperature results in more energy transfer to the peptide ion and less energy transfer to the surface.

B. Effect of Peptide Vibrational Temperature. As shown in Table 1 and Figure 1, increasing T_{vib} has the opposite effect compared to increasing T_{surf}. Though the changes in the average percent energy transfers are small with increases in T_{vib}, there are near-linear decreases and increases, respectively, in the energy transfers to ΔE_{int} and ΔE_{surf}. In addition, as shown in Figure 2 for the simulations at T_{vib} of 300 and 2000 K, there are corresponding small shifts in the peaks in $P(\Delta E_{int})$ and $P(\Delta E_{surf})$ to lower and higher values. With an increase in the peptide vibrational temperature, there is more energy transferred to the surface and less energy transferred to the peptide.

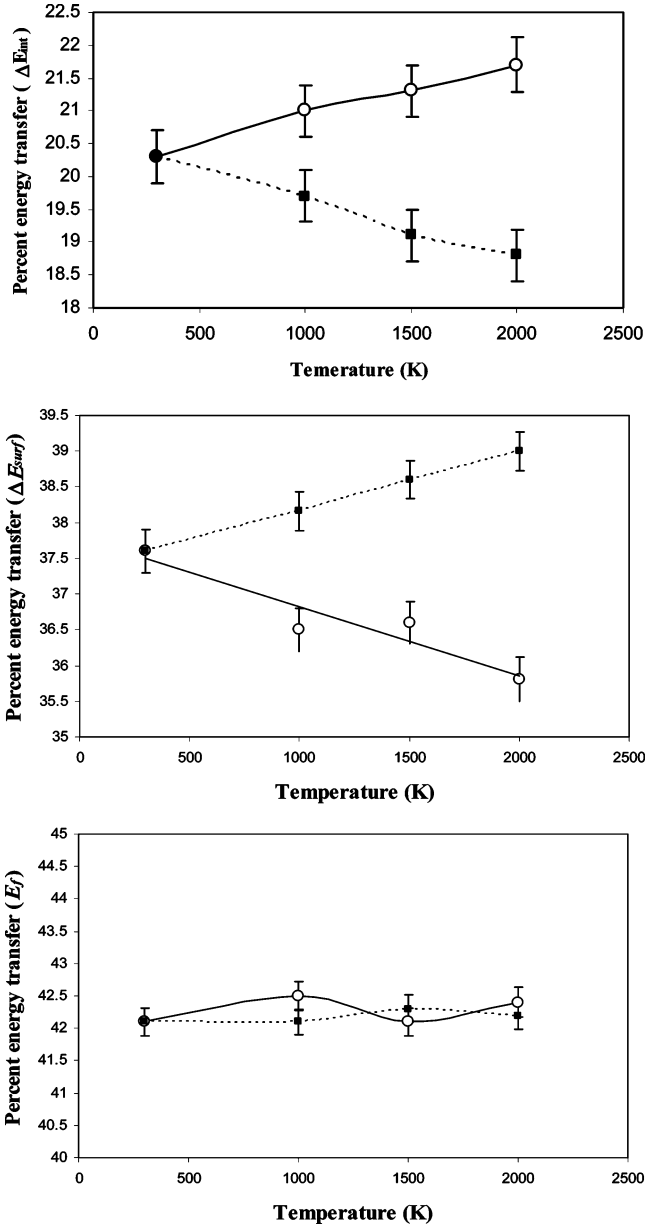

Figure 1. Plots of percent energy transfers versus T_{surf} (○) and T_{vib} (■). For the variable T_{surf} simulations, T_{vib} and T_{rot} of Gly_2-H^+ are kept at 300 K. T_{surf} and T_{rot} are kept at 300 K for the variable T_{vib} simulations.

The fraction of the 1614 kcal/mol collision energy transferred to Gly_2-H^+ internal energy decreases from 20.3% to 18.8% as the ion's initial temperature is increased from 300 to 2000 K. As discussed in section III, this temperature increase results in initial average Gly_2-H^+ internal energies of 94.5, 133.5, 172.2, and 214.9 kcal/mol for T_{vib} of 300, 1000, 1500, and 2000 K, respectively. The collision energy transferred to Gly_2-H^+ is 328−303 kcal/mol and is nearly independent of the ion's initial vibrational energy.

V. Summary

The major result from this study is that there are no significant changes in the energy transfer efficiencies for Gly_2-H^+ collisions with the diamond {111} surface as either the surface or Gly_2-H^+ vibrational temperature is varied. The latter is in accord with experimental results by Herman and co-workers.[43] This insen-

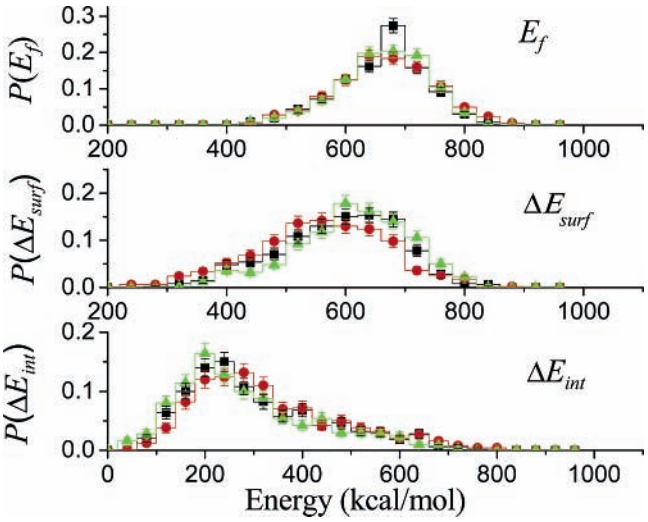

Figure 2. Distributions of energy transfer to the ion (ΔE_{int}) and to the surface (ΔE_{surf}) and of the energy remaining in translation (E_f) for Gly_2-H^+ collisions with the diamond {111} surface at T_{surf} and T_{vib} temperatures of 300 and 2000 K. T_{rot} is fixed at 300 K. The standard deviations are given as vertical lines. The results of simulations at T_{surf}, T_{vib} of (black ■) 300 K, 300 K; (red ●) 300 K, 2000 K; and (green ▲) 2000 K, 300 K are shown.

sitivity in the collisional energy transfer efficiencies is consistent with an impulsive model for surface-induced dissociation.[16]

A detailed analysis of the energy transfer efficiencies shows some small dependencies on the surface and Gly_2-H^+ vibrational temperatures. The energy remaining in projectile translation, E_f, does not depend on these temperatures, but the transfer to the surface, ΔE_{surf}, and to the projectile's internal degrees of freedom, ΔE_{int}, do. Thus, there seems to be some dynamical coupling between the surface and projectile vibrational energies but not with the projectile's translational energy. Increasing T_{surf} results in a small, near-linear increase and decrease, respectively, in the energy transfer to ΔE_{int} and ΔE_{surf}. The opposite is found when the Gly_2-H^+ vibrational temperature, T_{vib} is increased; that is, there is a near-linear decrease and increase in the respective transfers to ΔE_{int} and ΔE_{surf}. These are small effects, as shown in Figure 1, but they may assist in developing a model for energy transfer in SID.

Finally, it is of interest to consider the possible role of ZPE in the energy transfer dynamics reported here. Quasiclassical thermal initial conditions,[40] which include ZPE, were chosen for the Gly_2-H^+ ion. The surface's thermal initial conditions were chosen by a classical molecular dynamics (MD) simulation[41] which adds an average thermal energy of $3NRT$ to a harmonic surface model. In a previous study,[42] for which a small alkanethiolate self-assembled monolayer (H-SAM) surface model was used and its vibrational frequencies could be evaluated, it was found that, for temperatures of 0 and 300 K, quasiclassical and MD initial conditions for the surface give very similar energy transfer results. At 0 K, the surface is in its classical potential energy minimum for the MD initial conditions but contains ZPE for the quasiclassical initial conditions. At 293 K, the surface contains approximately a factor of 2 more energy by quasiclassical sampling as compared to MD sampling. These striking differences in the surface's energy for the MD and quasiclassical initial conditions had at most only a small effect on the energy transfer dynamics.[42] For the large diamond surface model used here, calculating its vibrational frequencies and performing quasiclassical sampling is impractical. However, the previous finding for the H-SAM surface suggests MD sampling for the diamond surface model should be adequate. As found in the work presented here, the overall insensitivity of the Gly_2-H^+ + diamond {111} collision energy transfer efficiencies on the surface temperature suggests that the method used to choose initial conditions for the surface, in simulations of peptide-H^+ + surface collisional energy transfer, is not a critical issue.

Classical trajectory simulations of bimolecular reactions, for example, $H + H_2 \rightarrow H_2 + H$,[44] unimolecular reactions,[45] and intramolecular vibrational energy redistribution (IVR)[46] have shown it is often necessary to include ZPE in the molecule to obtain agreement with the quantum dynamics. For this reason quasiclassical sampling, with ZPE included, was used for the Gly_2-H^+ ion. Its ZPE is 88.0 kcal/mol and is the principal contributor to the ion's average thermal internal energy at 300 K (i.e., this energy is 94.5, 133.5, 172.2, and 214.9 kcal/mol for the 300, 1000, 1500, and 2000 K simulations, respectively). Before the simulations were performed, it was difficult to predict the role of the Gly_2-H^+ ZPE on the energy transfer dynamics. For a statistical-type model, increasing the initial internal energy of Gly_2-H^+ with ZPE would decrease collisional energy to the Gly_2-H^+ vibrational modes. On the other hand, for nonstatistical energy transfer, adding ZPE and increasing the initial internal motion of Gly_2-H^+ might have increased energy transfer to Gly_2-H^+ vibration, as found for IVR from an excited C−H stretch mode of benzene to its remaining bath modes.[47] The simulation results indicate that the efficiency of collisional energy transfer to the Gly_2-H^+ ion's vibrational modes is overall insensitive to the ion's initial temperature (i.e., energy content), and apparently ZPE does not have an important effect on the energy transfer dynamics. In future work, it will be of interest to see if this is also the case for larger peptide-H^+ ions.

Acknowledgment. This material is based upon work supported by the National Science Foundation under Grant 0412677 and the Robert A. Welch Foundation under Grant D-0005. O.C. and C.S. were Detroit High School students, partially supported by the PRF-SEED program, which was managed by Keith Williams at Wayne State University. We thank Kihyung Song for many helpful and valuable discussions.

References and Notes

(1) Cooks, R. G.; Ast, T.; Mabud, M. A. *Int. J. Mass Spectrom.* **1990**, *100*, 209.
(2) Mabud, M. A.; Dekrey, M. J.; Cooks, R. G. *Int. J. Mass Spectrom.* **1985**, *67*, 285.
(3) Winger, B. E.; Laue, H. J.; Horning, S. R.; Julian, R. K.; Lammert, S. A.; Riederer, D. E.; Cooks, R. G. *Rev. Sci. Instrum.* **1992**, *63*, 5613.
(4) McCormack, A. L.; Somogyi, Á.; Dongre, A. R.; Wysocki, V. H. *Anal. Chem.* **1993**, *65*, 2859.
(5) Burroughs, J. A.; Wainhaus, S. B.; Hanley, L. *J. Phys. Chem.* **1994**, *98*, 10913.
(6) Wörgötter, R.; Grill, V.; Herman, Z.; Schwarz, H.; Märk, T. D. *Chem. Phys. Lett.* **1997**, *270*, 333.
(7) Cooks, R. G.; Ast, T.; Pradeep, T.; Wysocki, V. *Acc. Chem. Res.* **1994**, *27*, 316.
(8) Jones, J. L.; Dongre, A. R.; Somogyi, Á.; Wysocki, V. H. *Abstr. Pap. Am. Chem. Soc.* **1994**, *208*, 49.
(9) Meot-Ner, M.; Dongre, A. R.; Somogyi, Á.; Wysocki, V. H. *Rapid Commun. Mass Spectrom.* **1995**, *9*, 829.
(10) Dongre, A. R.; Jones, J. L.; Somogyi, Á.; Wysocki, V. H. *J. Am. Chem. Soc.* **1996**, *118*, 8365.
(11) Tsaprailis, G.; Nair, H.; Somogyi, Á.; Wysocki, V. H.; Zhong, W. Q.; Futrell, J. H.; Summerfield, S. G.; Gaskell, S. J. *J. Am. Chem. Soc.* **1999**, *121*, 5142.
(12) Lim, H. J.; Schultz, D. G.; Yu, C. W.; Hanley, L. *Anal. Chem.* **1999**, *71*, 2307.
(13) Schultz, D. G.; Lim, H.; Garbis, S.; Hanley, L. *J. Mass Spectrom.* **1999**, *34*, 217.
(14) Laskin, J.; Denisov, E.; Futrell, J. *J. Phys. Chem. B* **2001**, *105*, 1895.
(15) Laskin, J.; Futrell, J. H. *J. Chem. Phys.* **2002**, *116*, 4302.

(16) Schultz, D. G.; Wainhaus, S. B.; Hanley, L.; de Sainte Claire, P.; Hase, W. L. *J. Chem. Phys.* **1997**, *106*, 10337.

(17) Laskin, J.; Denisov, E.; Futrell, J. *J. Am. Chem. Soc.* **2000**, *122*, 9703.

(18) Laskin, J.; Byrd, M.; Futrell, J. *Int. J. Mass Spectrom.* **2000**, *196*, 285.

(19) Kubišta, J.; Dolejšek, Z.; Herman, Z. *Eur. Mass Spectrom.* **1998**, *4*, 311.

(20) Vekey, K.; Brenton, A. G.; Beynon, J. H. *J. Phys. Chem.* **1986**, *90*, 3569.

(21) Wysocki, V. H.; Kenttamaa, H. I.; Cooks, R. G. *Int. J. Mass Spectrom. Ion Processes* **1987**, *75*, 181.

(22) Hakansson, K.; Axelsson, J.; Palmblad, M.; Hakansson, P. *J. Am. Soc. Mass Spectrom.* **2000**, *11*, 210.

(23) Wainhaus, S. B.; Lim, H. J.; Schultz, D. G.; Hanley, L. *J. Chem. Phys.* **1997**, *106*, 10329.

(24) de Maaijer-Gielbert, J.; Somogyi, Á.; Wysocki, V. H.; Kistemaker, P. G.; Weeding, T. L. *Int. J. Mass Spectrom.* **1998**, *174*, 81.

(25) Morris, M. R.; Riederer, D. E.; Winger, B. E.; Cooks, R. G.; Ast, T.; Chidsey, C. E. D. *Int. J. Mass Spectrom.* **1992**, *122*, 181.

(26) Schultz, D. G.; Hanley, L. *J. Chem. Phys.* **1998**, *109*, 10976.

(27) Hanley, L.; Lim, H. J.; Schultz, D. G.; Wainhaus, S. B.; deSainteClaire, P.; Hase, W. L. *Nucl. Instrum. Methods B* **1997**, *125*, 218.

(28) Meroueh, O.; Hase, W. L. *Phys. Chem. Chem. Phys.* **2001**, *3*, 2306.

(29) Wang, J.; Meroueh, S. O.; Wang;, Y.; Hase, W. L. *Int. J. Mass Spectrom.* **2003**, *203*, 57.

(30) Žabka, J.; Dolejšek, Z.; Herman, Z. *J. Phys. Chem. A* **2002**, *106*, 10861.

(31) Cornell, W. D.; Cieplak, P.; Bayly, C. I.; Gould, I. R.; Merz, K. M.; Ferguson, D. M.; Spellmeyer, D. C.; Fox, T.; Caldwell, J. W.; Kollman, P. A. *J. Am. Chem. Soc.* **1995**, *117*, 5179.

(32) Meroueh, S. O.; Wang, Y.; Hase, W. L. *J. Phys. Chem. A.* **2002**, *106*, 9983.

(33) Laskin, J.; Futrell, J. H. *J. Chem. Phys.* **2003**, *119*, 3413.

(34) Meroueh, O.; Hase, W. L. *J. Am. Chem. Soc.* **2002**, *124*, 1524.

(35) Hass, K. C.; Tamor, M. A.; Anthony, T. R.; Banholzer, W. F. *Phys. Rev. B* **1992**, *45*, 7171.

(36) Meroueh, O.; Hase, W. L. *J. Phys. Chem. A* **1999**, *103*, 3981.

(37) Hase, W. L.; Duchovic, R. J.; Hu, X.; Komornicki, A.; Lim, K. F.; Lu, D.-h.; Peslherbe, G. H.; Swamy, K. N.; Vande Linde, S. R.; Zhu, L.; Varandas, A.; Wang, H.; Wolf, R. J. *QCPE* **1996**, *16*, 671.

(38) Chapman, S.; Bunker, D. L. *J. Chem. Phys.* **1975**, *62*, 2890.

(39) Cho, Y. J.; Vande Linde, S. R.; Zhu, L.; Hase, W. L. *J. Chem. Phys.* **1992**, *96*, 8275.

(40) Peslherbe, G. H.; Wang, H. B.; Hase, W. L. *Adv. Chem. Phys.* **1999**, *105*, 171.

(41) Allen, M. P.; Tildesley, D. J. *Computer Simulation of Liquids*; Oxford University Press: New York, 1987.

(42) Yan, T.-Y.; Hase, W. L. *J. Phys. Chem. B* **2002**, *106*, 8029.

(43) Qayyum, A.; Herman, Z.; Tepnual, T.; Mair, C.; Matt-Leubner, S.; Scheier, P.; Märk, T. D. *J. Phys. Chem. A* **2004**, *108*, 1.

(44) Aoiz, F. J.; Bañares, L.; Herrero, V. J. In *Advances in Classical Trajectory Methods, Vol. 3, Comparisons of Classical and Quantum Dynamics*; Hase, W. L., Ed.; JAI Press: London, 1998; p 121.

(45) Grebenschchikov, S. Y.; Schinke, R.: Hase, W. L. In *Comprehensive Chemical Kinetics*, Part 1. The Reaction Step; Green, N. J. B., Ed.; Elsevier: Amsterdam, 2003; p 105.

(46) Baer, T.; Hase, W. L. *Unimolecular Reaction Dynamics. Theory and Experiments*; Oxford: New York, 1996; p 84.

(47) Lu, D.-H.; Hase, W. L. *J. Chem. Phys.* **1989**, *91*, 7490.